River Flow 2010 - Dittrich, Koll, Aberle & Geisenhainer (eds) - © 2010 Bundesanstalt für Wasserbau ISBN 978-3-939230-00-7

Evaluation of Bed Shear Stress from Velocity Measurements in Gravel-Bed River with Local Non-Uniformity

A. Tominaga & T. Sakaki
Department of Civil Engineering, Nagoya Institute of Technology, Nagoya, Japan

ABSTRACT: Field measurements of turbulent open-channel flow were performed in a gravel-bed river with local non-uniformity. The velocity distributions and turbulent structures were measured by using ADV in a river with riverside embayment and another river with a group of groynes. The local bed shear stress was evaluated by data fitting methods for the distributions of the log-law, Reynolds stress and turbulence intensities. The data obtained by these three methods indicated almost similar values but some differences were recognized among them. The differences are attributed to the effects of ADV noise, boundary conditions and local flow structures. The turbulence structures in these non-uniform flow fields conform to the universal characteristics in two-dimensional open-channel flows. The mean and turbulent velocities obtained by ADV are reasonably accurate for evaluating turbulence characteristics and bed shear stress.

Keywords: field measurement, ADV, bed shear stress, resistance, turbulence structure, roughness

1 INTRODUCTION

There are many approaches to improve ecological environment by creating diversity of river configuration in straightened rivers. As measures to create flow diversity, riverside embayment and groynes were often constructed. The riverside embayment provides a dead water zone for aquatic-life habitat but the sand filling and the degradation of water quality are concerned (Tominaga et al. 2009). Groynes are expected to create deep scours at their head zones and to make sand bars in their downstream zones but the stability of themselves and impacts of bed deformation on river courses become problems (Tominaga & Matsumoto 2006). In order to predict changes of river-bed form and flow structures, numerical simulations become a powerful tool. For accurate application of the numerical methods, it is necessary to understand resistance characteristics in actual rivers. The Manning's roughness coefficient, the Darcy-Weisbach's friction coefficient or the equivalent grain roughness is usually used according to an employed resistance law in 2D or 3D flow calculations. It is necessary to determine the resistance coefficient corresponding to local conditions of the bed material. The estimation of the local bed shear stress becomes essential to estimate such resistance coefficients in rivers.

For this purpose, we performed field measurements of velocity by using Acoustic Doppler Velocimeter (ADV) in two typical river sites that river improvement works were conducted recently. One is a site of newly constructed embayment zone in the Yada River. After construction of the embayment, a large accumulation of sand and gravel occurred in the embayment zone. The other is a site around the groynes in the Shonai River. In this area, a scoured region was generated near the head of the most upstream groyne.

The applicability of turbulence measurements by using ADV in actual rivers and laboratory flumes were verified by many researchers (e.g. Nikora & Goring 2000, Kim et al. 2000, Song & Chiew 2001, Storm & Papanicolaou 2007). It was also proved in the present study that the velocity measurements using ADV are reasonably accurate and the turbulence structures have constancy even in these non-uniform flow fields. Therefore, we tested several methods of evaluating friction velocity by using mean velocity and turbulence statistics values and considered the resistance characteristics in the non-uniform river flows.

2 FIELD OBSERVATION

2.1 *The Yada River Site*

The embayment in the Yada River was constructed on the right bank of the main channel on March 2008. The main channel at the target site is almost straight, 30m in width and about 1/800 in slope. The open-mouth length is 100m and lateral depth is 25m at the bottom, and 140m and 35m respectively at the level of the flood plain. A rhombus-shaped deflector made by riprap is set at the upstream side near the open mouth. Its length is 10m, width is 5m and height is 0.8m from the initial bed level.

We measured bed profile around the embayment four times by using a total station. Figure 1 shows the bed elevation contours and measured depth-averaged velocity vectors on November 5, 2008. The bed configuration was changed by repeated floods. After 4 months from the construction, significant sand bar was created behind the deflector. The bed form was extremely changed after experienced over-bank floods at the end of August. The deposition area was extended to the upstream end and the embayment side. The upstream mouth of the embayment was completely closed at an ordinary water level. The deep area in the embayment was reduced but the left-bank deep area developed. The measurement sections were set at x = 0m, 80m and 160m in transverse direction. Bed profiles at the measurement sections are shown in Figure 2. Grain size distributions were measured at the several sampling points along the velocity measurement sections.

2.2 *The Shonai River Site*

The group of groyne was constructed along the right bank of the Shonai River on March 2009. The groyne was composed of buildup of crushed stone covered by metal mesh and the length is 20m, the width is 3 - 5m and the height is 1.5m from the bed level. Eight groynes were set at 60m interval on right bank side. We concentrated on the flow around the first groyne. The bed configuration and the measurement points are shown in Figure 3. A deep scour region is recognized around the head of the first groyne. The measurement sections were set at x = -25m, 20m and 60m as surrounding the deep region where the flow depth is less than 1m. The velocity was measured in the same manner as conducted in the Yada River. The depth-averaged velocity vectors are also shown in Figure 3. The grain size distribution was measured at the velocity measurement points in Figure 3.

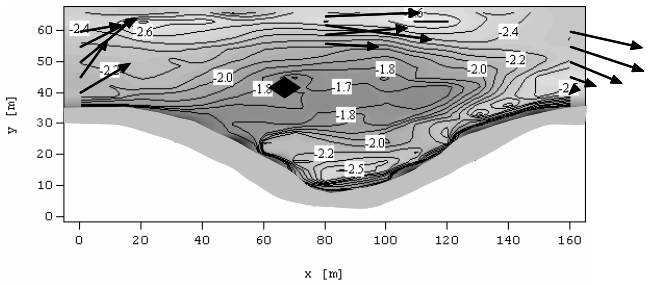

Figure 1 Bed contours and measured velocity vectors in the Yada River in the Yada River

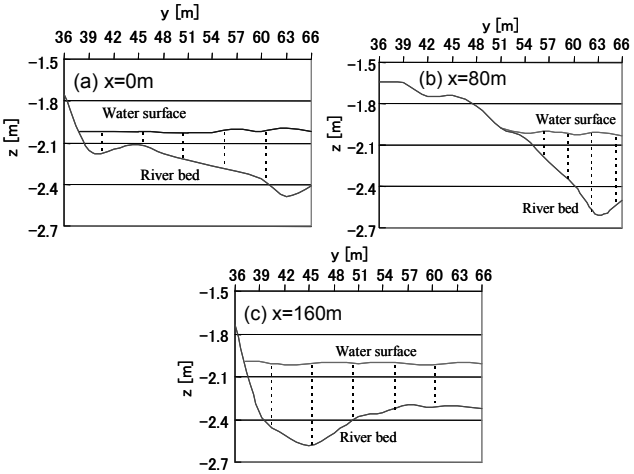

Figure 2 Bed profiles at the measurement section

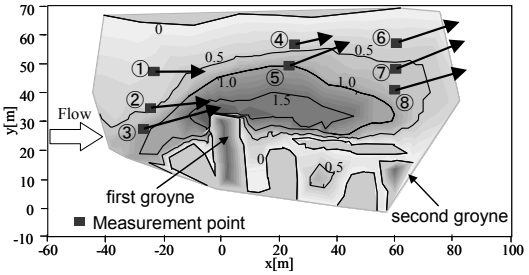

Figure 3 Bed configuration and the measurement points in the Shonai River

2.3 *Velocity Measurement Procedure*

The vertical distributions of velocity were measured by using ADV (NorTec Inc.). The ADV was attached on a pole movable vertically along a support platform. The prove orientation was set to be perpendicular to the normal cross section of the river. We set the primary axis as the x direction so that the lateral mean velocity becomes zero at each point. The sampling frequency was 20Hz in the Yada River and 25Hz in the Shonai River. The sampling time was 205s and 164s, respectively. In considering that a bursting period in open-channel flows is 1.5 - 3 times of a flow depth divided by a maximum velocity (Nezu & Nakagawa 1993), a dominant turbulence time-scale is almost 3-6 seconds. As long as there is no lateral large-scale motion, the sampling time is enough for calculating statistical values of turbulent flow.

It is well known that the turbulence data obtained by ADV has some high-frequency noise (Nikora & Goring 1998, Garcia et al. 2005). Gar-

cia et al. (2005) proposed a parameter, $F = Lf_R / U_c$, where L = length scale of energy containing eddies, f_R = ADV frequency (f_R=25Hz or 20Hz) and U_c=convection velocity. Here a water depth h and a mean velocity $\overline{u}$ were taken as L and U_c, respectively. For high values of F, $F > 20$, the ADV is able to describe the turbulent flow, but for lower values, $F < 20$, the ADV does not resolve the turbulent motion. In this study, only two points were not satisfy this condition of $F > 20$ at (x=0m, y=40m and 45m) in the Yada River. In this study, the noise was observed in the measured data from power spectrum analyses. When the high-frequency noise was removed by filtering, filtered turbulence intensities reduced about 3 - 4 percent from the raw data.However, raw velocity signals of ADV were used for analysis without processing. The noise effects were only accounted by checking the appearance of obtained results.

3 EVALUATION METHOD OF BED SHEAR STRESS

The local bed shear stress can be evaluated from velocity measurements by using various methods (e.g. Smart 1999, Kim et al. 2000, Song& Chiew 2001, Piedra et al. 2009). In this study, three methods were employed by using vertical distributions of the primary mean velocity, the shear Reynolds stress and the turbulence intensity. Although these methods are valid for 2D prismatic open-channel flows, we tested their applicability for the present local non-prismatic flows. The friction velocity is considered in this study instead of the bed shear stress for simplicity. Each method is described as follows.

1) Evaluation method by log-law

The log-law equation is expressed as follows on a completely rough bed.

$$\frac{U}{u_*} = \frac{1}{\kappa}\ln\left(\frac{z}{k_s}\right) + B \tag{1}$$

where U = primary mean velocity, u_* = friction velocity, κ = von Karman constant, z = vertical coordinate, k_s = equivalent grain roughness, and B = integration constant. The origin of the z coordinate was set to the roughness top by reference to the scale reading of the acoustic sensor. The bed shift to the virtual origin was not considered because of the difficulty of distinguishing the roughness arrangement in the field. As to the constants, we adopted $\kappa = 0.41$ according to Nezu & Nakagawa (1986) and $B = 8.5$ from Graf (1998). The applicable region of the log-law is usually $z/h < 0.2$ for smooth bed but, in the present cases, it covered up to the free surface without a wake region. The equation (1) is rearranged to

$$U = \frac{u_*}{\kappa}\ln z + Bu_* - \frac{u_*}{\kappa}\ln k_s \tag{2}$$

From the measured velocity profile, we obtain a linear regression equation on semi-logarithmic plotting

$$U = A\ln z + C \tag{3}$$

By comparing equation (2) with (3), the friction velocity and the equivalent grain roughness are obtained as

$$u_* = \kappa A \tag{4}$$

$$k_s = \exp\left\{(Bu_* - C)\frac{\kappa}{u_*}\right\} \tag{5}$$

2) Evaluation method by Reynolds stress $-\overline{uw}$

In a two-dimensional open-channel flow with high Reynolds number, the Reynolds stress $-\overline{uw}$ is distributed linearly from zero at the free surface to the bed shear stress at the bed as

$$\frac{-\overline{uw}}{u_*^2} = 1 - \frac{z}{h} \tag{6}$$

where u, w=turbulent fluctuating velocities in x and z directions, respectively. The friction velocity can be evaluated by extrapolating the measured Reynolds stress to the bed. This value of friction velocity is designated as u_{*t}. It is regarded that the distribution of the Reynolds stress is liable to be affected by secondary currents and form drag due to roughness elements (Nikora et al. 2007).

3) Evaluation method by turbulence intensity

It is well known that the turbulence intensities follow the universal profiles proposed by Nezu & Nakagawa (1993) in 2-dimensional open-channel flows

$$\frac{u'}{u_*} = 2.30\exp\left(-\frac{z}{h}\right) \tag{7}$$

$$\frac{v'}{u_*} = 1.63\exp\left(-\frac{z}{h}\right) \tag{8}$$

$$\frac{w'}{u_*} = 1.27\exp\left(-\frac{z}{h}\right) \tag{9}$$

where $u' = \sqrt{u^2}$, $v' = \sqrt{v^2}$ and $w' = \sqrt{w^2}$ = turbulence intensities in the x, y and z directions, respectively. We can evaluate the local friction velocity from this relation. The value of friction velocity evaluated by data fitting to the equation

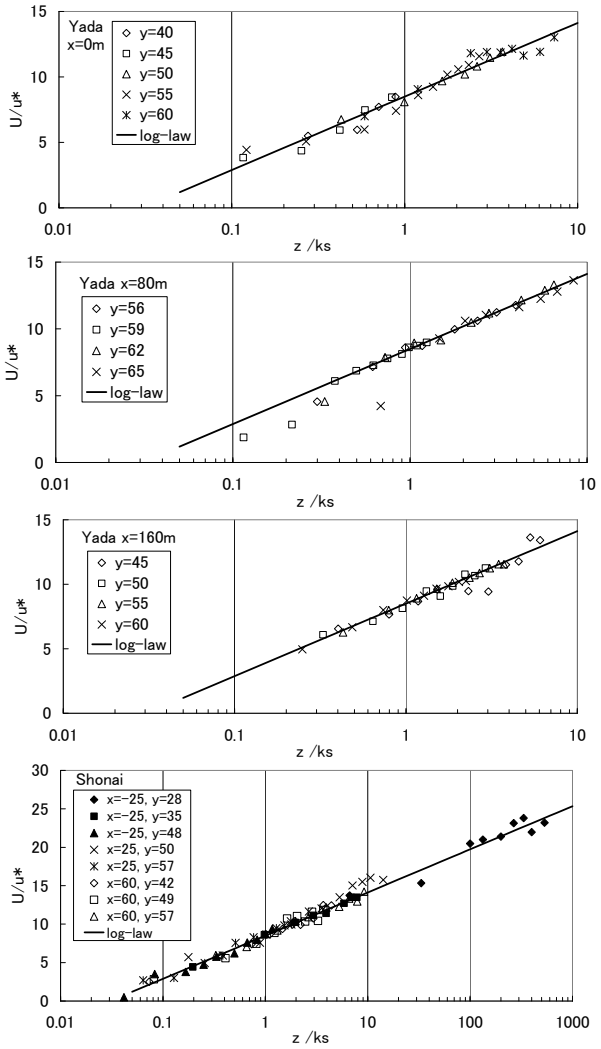

Figure 4 Vertical distribution of primary mean velocity with log-law

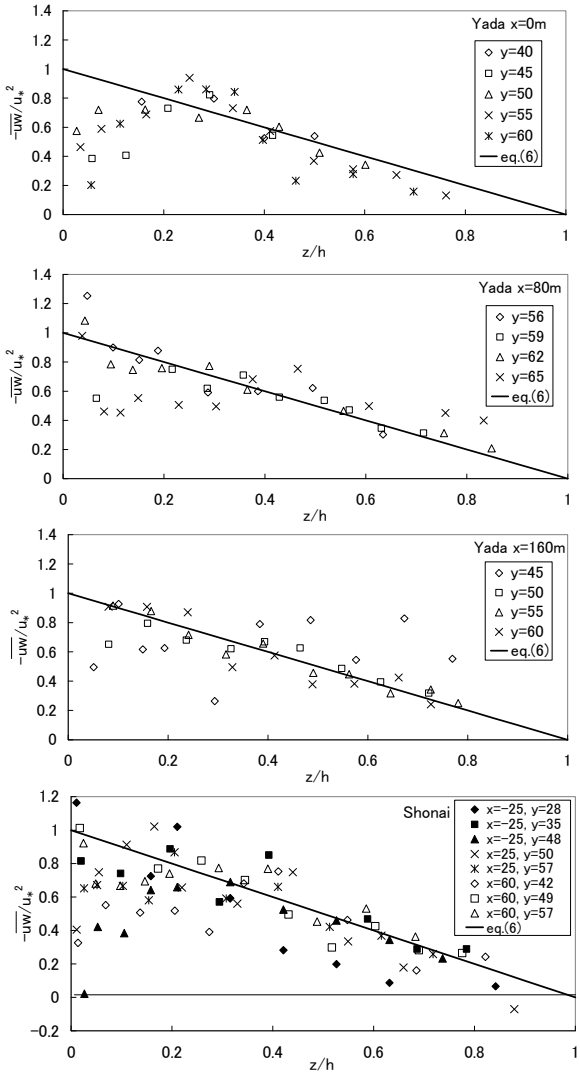

Figure 5 Vertical distribution of Reynolds stress $-\overline{uw}$

(7) is designated as u_{*r}. A streamwise component was used for the evaluation though all three components were obtained in the ADV measurements. This is because the streamwise components can be easily measured in comparison with the other components in many cases.

4 RESULTS AND DISCUSSION

4.1 *Universal Characteristics of Turbulence in Open Channel Flow*

At first, the applicability of universal distributions of turbulence quantities was investigated. Then the evaluation of friction velocity was conducted by using the above three methods. The vertical distributions of primary mean velocity are shown in Figure 4 for each measured section. The solid line in the figure is the log-law profile of equation (1). The primary direction was defined as an average of the direction at each measuring height and instantaneous velocity components were recalculated by coordinate conversion in horizontal plane. The friction velocity u_* and the equivalent grain roughness k_s were calculated by applying a regression analysis. The velocity and vertical distance in these figures are normalized by these values. The obtained values are shown in Tables 1 and 2. It is recognized that the log-law distribution is applicable in almost all sections. The section of x = 0m in the Yada River is just upstream the sand bar and the flow is turning toward the left bank. The flow depth is small and the secondary currents are significant in this section. The velocity here tends to be inflected near the bed. At the section of x = 80m, the flow is concentrated on the left bank and the flow depth becomes larger. The velocity near the bed tends to depart from the log-law. At the section of x = 160m in the Yada River and at all sections in the Shonai River, the velocity profiles show good agreement with the log-law over the whole flow depth.

Figure 5 show the vertical distribution of the Reynolds stress $-\overline{uw}$ normalized by evaluated u_{*t}. The profiles of $-\overline{uw}$ are rather scattered because of the difficulty and the short-time of the measurement. At the section of x = 0m in the Yada river, the Reynolds stress profiles depart

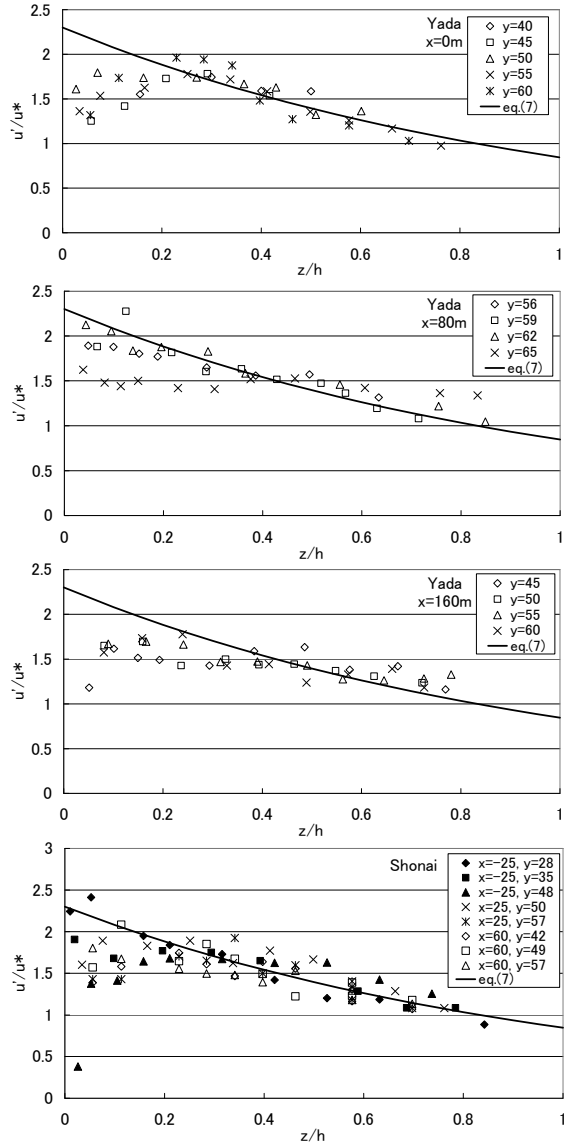

Figure 6 Vertical distribution of turbulence intensity u'

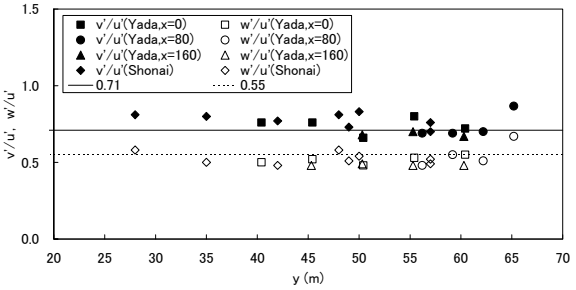

Figure 7 Ratio of turbulence intensities

from the linear distribution near the bed and near the free surface, and attain the peak at about z/h = 0.3. The profiles do not follow the triangular distribution at the points of (x=80m, y=65m) and (x=160m, y=45m). It is difficult to evaluate the friction velocity from the Reynolds stress in these regions. The former is affected by the left bank and the latter is near the separated flow area behind the sand bar. Except for these points, the profiles at x = 80m and 160m almost fit the triangular distribution.

In the section of the Shonai River, the data spread becomes larger than the sections in the Yada River. At relatively deep points, (x=-25m, y=28m) and (x=25m, y=50m), the Reynolds stress becomes small near the free surface. This corresponds to the reduction of the mean-velocity near the free surface. At relatively shallow points, (x=-25m, y=48m) and (x=25m, y=57m), the values become small near the bed. Except for these sections, the profiles fit the triangular distribution though they oscillate around the theoretical line.

The distributions of turbulence intensity u' normalized by u_{*_r} are shown in Figure 6. The compatibility of the measured data to the universal equation (7) is almost similar to that of the Reynolds stress. However, the distribution of the turbulence intensity is rather steady and the degree of agreement between measurement data and the equation is reasonably high in the region apart from the bed. The value near the bed becomes small characteristically in rough-bed flows. In the section of x = 80m in the Yada River, the decrease near the bed is not significant except y = 65m. In the section of x = 160m, profiles become nearly constant in the vertical direction. In any case, the local friction velocity can be evaluated from turbulence intensity in the region $z/h > 0.2$.

The turbulence intensities, v' and w', showed similar profile as u'. As to the magnitude, the ratios of the depth-averaged turbulence intensities, $\overline{v'}/\overline{u'}$ and $\overline{w'}/\overline{u'}$ are shown in Figure 7 in all cases. From the equations (7) to (9), the following relations are obtained.

$$\overline{v'}/\overline{u'} = 0.71 \tag{10}$$

$$\overline{w'}/\overline{u'} = 0.55 \tag{11}$$

These ratios indicate almost similar value as equations (10) and (11) in all cases. As a result, the universal anisotropic characteristics of turbulence intensities are robustly recognized. However, it should be noticed that the values of turbulence intensities involve the ADV noise effects.

4.2 *Evaluation of Friction Velocity*

The values of friction velocity evaluated from the measured data by applying the above three methods are shown in Tables 1 and 2. In the table, typical grain size d_{50} and d_{90} obtained by screening test are also shown and U_m is the depth averaged primary mean velocity. Manning's roughness n_1 and the friction coefficient for Darcy-Weisbach formula, f_1, were calculated from u_* as

$$n_1 = \frac{h^{1/6}}{\sqrt{g}}\left(\frac{u_*}{U_m}\right) \tag{12}$$

$$f_1 = 8\left(\frac{u_*}{U_m}\right)^2 \tag{13}$$

Table 1 Measured and evaluated values (The Yada River)

x [m]	0	0	0	0	0
y [m]	40	45	50	55	60
h [m]	0.10	0.12	0.23	0.30	0.43
d_{50} [mm]	3.1	3.1	6.9	6.9	4.2
d_{90} [mm]	13.5	13.5	26.5	26.5	13.5
U_m [cm/s]	20.2	19.7	26.9	23.8	13.9
u_* [cm/s]	2.85	2.68	2.59	2.60	1.26
n_1	0.031	0.031	0.024	0.029	0.025
f_1	0.159	0.148	0.074	0.096	0.066
k_s [mm]	56.5	59.3	37.7	84.7	40.9
u_{*t} [cm/s]	2.70	2.90	2.36	2.86	1.79
u_{*r} [cm/s]	3.07	3.03	2.60	3.05	1.77

x [m]	80	80	80	80	160	160	160	160
y [m]	56	59	62	65	45	50	55	60
h [m]	0.20	0.35	0.53	0.66	0.52	0.32	0.31	0.31
d_{50} [mm]	7.6	11.9	11.9	4.6	1.0	1.0	8.3	8.3
d_{90} [mm]	22.0	38.0	38.0	16.0	9.0	9.0	22.0	22.0
U_m [cm/s]	20.7	30.0	40.6	35.5	10.0	19.8	26.9	25.8
u_* [cm/s]	2.02	4.21	3.67	2.74	0.92	2.10	2.69	2.95
n_1	0.024	0.038	0.026	0.023	0.026	0.028	0.027	0.030
f_1	0.076	0.158	0.065	0.048	0.068	0.090	0.083	0.105
k_s [mm]	32.1	201.0	69.3	36.7	65.9	79.3	64.8	100.6
u_{*t} [cm/s]	1.74	3.03	3.41	3.83	0.96	1.48	1.84	2.22
u_{*r} [cm/s]	2.05	3.23	3.43	3.93	1.48	1.88	2.37	2.78

Table 2 Measured and evaluated values (The Shonai River)

x [m]	-25	-25	-25	25	25	60	60	60
y [m]	28	35	48	50	57	42	49	57
h [m]	0.95	0.51	0.38	0.91	0.39	0.73	0.58	0.41
d_{50} [mm]	14.8	12.1	19.0	20.0	14.4	36.3	15.1	11.7
d_{90} [mm]	46.0	28.5	51.0	42.0	36.0	57.0	46.0	36.0
U_m [cm/s]	28.1	21.2	20.5	24.1	15.3	27.9	26.5	23.8
u_* [cm/s]	1.30	1.84	2.84	1.74	1.83	2.75	2.70	1.93
n_1	0.015	0.025	0.038	0.023	0.033	0.030	0.030	0.022
f_1	0.017	0.060	0.153	0.042	0.114	0.078	0.083	0.053
k_s [mm]	1.5	51.0	240.2	56.4	156.1	135.8	122.3	30.4
u_{*t} [cm/s]	1.63	1.88	2.94	1.71	1.44	2.60	2.33	1.65
u_{*r} [cm/s]	2.01	1.88	2.68	2.28	1.60	3.30	2.80	2.32

The evaluated friction velocities u_*, u_{*t} and u_{*r} are compared in Figure 8. The section-average values $\overline{u}_*$, $\overline{u}_{*t}$ and $\overline{u}_{*r}$ are shown in Table 3. The average values of three kinds of friction velocities show reasonably good agreement in all sections, but considerable differences are recognized in some cases. In the total average, $\overline{u}_{*r}$ gives largest value and $\overline{u}_{*t}$ does smallest. The ADV noise tends to increase the turbulence intensity but the effect on the Reynolds stress is not apparent. This needs further investigation.

In the section of x = 0m of the Yada River, the lateral distributions are almost similar. At y = 55m and 60m, u_* obtained from the log-law becomes smaller than others. In the section of x = 80m, the values of $\overline{u}_{*t}$ and $\overline{u}_{*r}$ are almost equal, but u_* shows different distribution at y = 59m and y = 65m. It is considered that the friction of the left bank increases turbulence but decrease the mean velocity at y = 65m. The reason why u_* at y = 59m becomes large is uncertain. It may be related

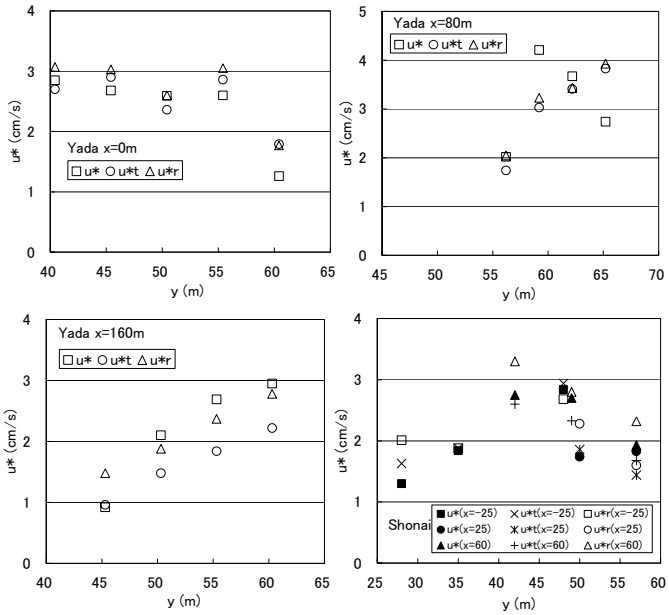

Figure 8 Comparison of friction velocities evaluated by three methods

Table 3 Section averaged friction velocity

Section	$\overline{u}_*$ (m/s)	$\overline{u}_{*_t}$ (m/s)	$\overline{u}_{*_r}$ (m/s)
Yada (x=0m)	0.024	0.025	0.027
Yada (x=80m)	0.032	0.030	0.032
Yada (x=160m)	0.022	0.016	0.021
Shonai (x=-25m)	0.020	0.022	0.022
Shonai (x=25m)	0.018	0.016	0.019
Shonai (x=60m)	0.025	0.022	0.028

with that the large grain size and contracting and accelerating flow conditions in this region. When the bed roughness is large, the definition of the vertical-coordinate origin becomes problem. In the section of x = 160m, $\overline{u}_{*t}$ obtained from the Reynolds stress underestimated at $y \geq$ 50m in comparison with the other two methods. In this area, the flow is diverging and the flow depth is decreasing from narrow and deep section. These effects may have caused the reduction of the Reynolds stress, but it should be investigated furthermore. In the Shonai River case, the agreement among three kinds of friction velocity is also recognized. Particularly, $\overline{u}_*$ and $\overline{u}_{*t}$ are coincide with each other, but $\overline{u}_{*r}$ tends to be higher than these two.

It is concluded that the three methods evaluating friction velocity employed in this study are reasonably acceptable. This fact means that the velocity and turbulence measurement by using ADV has fairly good accuracy even though field observations include various measurement errors. It is also verified that the self-similarity of turbulence in open channel flows is established in these non-uniform flow conditions. However, the values of three types show considerable disagreement in some regions. The log-law method is most popular for estimating the friction velocity. The appli-

cability of the log-law distribution for the primary mean velocity is reasonable except for the separating flow regions. However, the velocity gradient is sensitive to the shift of the profile origin. The measurement of the Reynolds stress distribution is rather difficult in field because it is liable to be affected by various local flow structures. The distribution of turbulence intensity u' can provide useful information more easily than the Reynolds stress in field measurements.

Although these three values agree with each other, the real value of the friction velocity has been unknown yet. These are only possible measures of understanding the resistance characteristics of the flow in fields.

4.3 *Resistance Characteristics*

The purpose of estimating the friction velocity is to obtain the resistance characteristics of the target flow. As the resistance parameter, Manning's roughness n, Darcy-Weisbach's friction coefficient f and the equivalent grain roughness k_s are considered. In numerical simulations of open channel flows, any one of resistance parameter is given. For depth-averaged calculation, n or f is usually provided. For three-dimensional calculation, k_s is sometimes used as a boundary condition. If the log-law is established over the whole flow depth, k_s is related to the velocity factor U_m / u_* as

$$\frac{U_m}{u_*} = \frac{1}{\kappa}\ln\left(\frac{h}{k_s}\right) + B - \frac{1}{\kappa} \tag{14}$$

The values of n or f are related to k_s by substituting equation (14) for $U_m / \overline{u}_*$ in the equations (12) and (13). The calculated n and f are plotted against h/k_s in Figure 9 and 10, respectively. The calculated friction coefficients coincide with the equation. This implies that the log-law distribution is well established over the whole flow depth in the present observation. The Manning's roughness is not a unique function of h/k_s depending on the flow depth as $h^{1/6}$. The values of n become almost constant in the region $h/k_s > 6.0$ and n = 0.23 - 0.26 can be adopted as a representative roughness value in these flow fields. It is noticed that the Manning's roughness increases with a decrease of h/k_s when h/k_s <6.0.

A problem is to determine the equivalent grain roughness k_s from the bed material condition. The equivalent grain roughness is useful as a boundary condition in 3D numerical calculations. Figure 11 shows the relation between equivalent grain roughness and the bed material size d_{90}. The values of k_s scatter widely ranging from $k_s = 1.4d_{90}$ to $k_s = 4.5d_{90}$. It is not easy to determine k_s directly from d_{90}. The distribution of grain size and the flow condition may affect the estimation of the equivalent grain roughness.

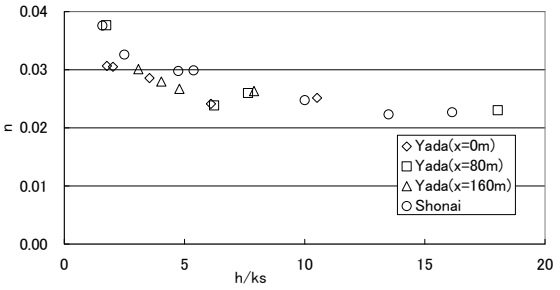

Figure 9 Manning's roughness

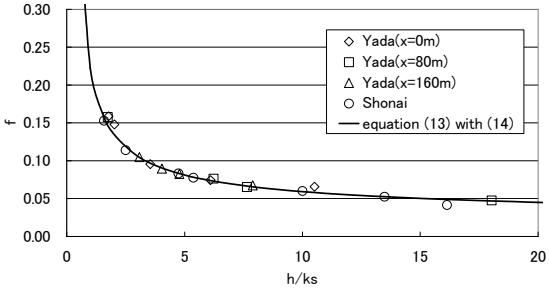

Figure 10 Friction coefficient

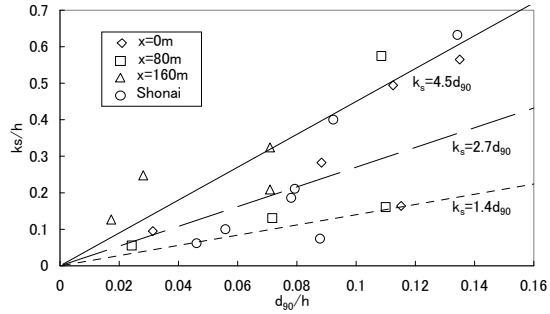

Figure 11 Relation between equivalent grain roughness k_s and bed material size d_{90}

4.4 *Spectral Analysis and Dissipation Rate*

Power spectra of primary turbulent velocity u were calculated by FFT methods at every point. Figure 12 shows an example of a power spectrum S_u against frequency f_r (Hz). It is recognized that the Kolmogoroff's -5/3 power law is applicable in the inertial sublayer. In the region 5Hz < f_r < 10Hz, the ADV noise is observed, but it does not influence the line fitting of -5/3 power law. The -5/3 power law can be applied at almost all points except for (x=0m, y=45m) section of the Yada River and some points very near the bed.

In the inertial sublayer of power spectrum, the following equation is obtained.

$$S_u = \frac{A}{(2\pi)^{2/3}}\overline{u}^{2/3}\varepsilon^{2/3}f_r^{-5/3} \tag{15}$$

where A is a constant and approximately A = 0.5. The dissipation rate ε can be evaluated from this equation. The vertical distributions of ε are shown in Figure 13 for the Shonai River. A curve in this figure is a semi-empirical formula proposed by Nezu & Nakagawa(1993).

$$\frac{\varepsilon h}{u_{*r}^3} = E_1 (z/h)^{-1/2} \exp(-3z/h) \qquad (16)$$

where E_1 is a constant and $E_1 = 8.43$ is taken here. The vertical profiles of ε are almost similar to the equation (16). The magnitude of ε is reasonable though it is smaller in the region z/h < 0.3. The small value of ε near the bed is possibly attributed to the roughness effects. As a result, turbulence measurements by using ADV provide reasonable fluctuation of velocity.

5 CONCLUSIONS

Turbulence measurements were performed in non-uniform gravel-bed rivers in order to understand the resistance characteristics of rivers. It was confirmed that the ADV measurement has a reasonable accuracy for both mean and fluctuating velocities. It is also verified that the self-similarity of turbulence in open channel flows is established in these non-uniform flow conditions. The friction velocity was evaluated by data fitting methods for the distributions of the log-law, the Reynolds stress and the turbulence intensities. The values of friction velocity evaluated by these three methods show reasonable agreement but some differences were recognized among them due to the effects of ADV noise, boundary conditions and flow structures.

The applicability of the log-law distribution for the primary mean velocity is reasonable except for the separating flow regions. The distribution of turbulence intensity u' can provide useful information more easily than the Reynolds stress in field measurements. The dissipation rate could be evaluated from power spectra of primary velocity. However, ADV noise effects must be investigated furthermore. These results provide useful suggestions to the expression of bed-roughness condition for 2D or 3D numerical simulations for river flow and sedimentation.

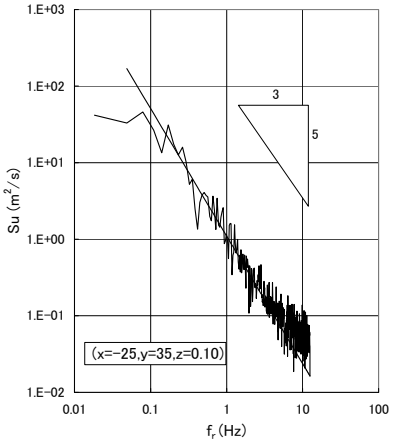

Figure 12 Example of spectral distribution of u

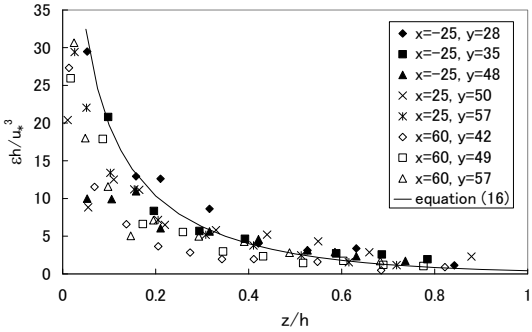

Figure 13 Vertical distribution of dissipation rate ε

REFERENCES

Bradshaw, P. 1967. Conditions for the existence of an inertial subrange in turbulent flow, A.R.C., R.&M., London, No.3603.

Garcia, C. M., Cantero, M. I., Niño, Y.; and García, M. H. 2005. Turbulence Measurements with Acoustic Doppler Velocimeters. Journal of Hydraulic Engineering, 131, 12, 1062-1073.

Graf, W. H. 1998. Fluvial Hydraulics. Flow and transport processes in channels of simple geometry. J Wiley & Sons, UK.

Kim, S. C., Friedrichs, C. T., Maa, J. P.-Y.and Wright, L. D. 2000. Estimating Bottom Stress in Tidal Boundary Layer from Acoustic Doppler Velocimeter Data. Journal of Hydraulic Engineering, ASCE, 126, 6, 399-406.

Nezu, I. and Nakagawa, H. 1993. Turbulence in Open Channel Flows, IAHR Monograph, Balkema.

Nikora V. and Goring, D. G. 1998. ADV Measurements of Turbulence: Can We Improve Their Interpretation? Journal of Hydraulic Engineering, 124, 6, 630-634.

Nikora V. and Goring, D. G. 2000. Flow Turbulence over Fixed and Weakly Mobile Gravel Beds. Journal of Hydraulic Engineering, 126, 9, 679-690.

Nikora, V., McLean, S., Coleman, S., Pokrajec, D., McEwan, I., Campbell, L., Aberle, J., Clunie, D. and Koll, K. 2007. Double-Averaging Concept for Rough-Bed Open-Channel and Overland Flows: Applications. Journal of Hydraulic Engineering, 133, 8, 884-895.

Piedra, M. M., Haynes, H. and Ervine, A. 2009. Review of Approaches to Estimating Bed Shear Stress From Velocity Profile Measurements. 33rd IAHR Congress, Vancouver. 2280-2287.

Song, T. and Chiew, Y. M. 2001. Turbulence Measurement In Nonuniform Open-Channel Flow Using Acoustic Doppler Velocimeter (ADV). Journal of Engineering Mechanics, 127, 3, 219-232.

Smart, G. M. 1999, Turbulent velocity profiles and boundary shear in gravel bed rivers, Journal of ydraulic Engineering, 125, 2, 106-116.

Strom, K. B. and Papanicolaou, A. N. 2007. ADV Measurements around a Cluster Microform in a Shallow Mountain Stream. Journal of Hydraulic Engineering, 133, 12, 1379-1389.

Tominaga, A., Jefung, J. and Sakaki, T. 2009. Sediment Transport around an Artificial Embayment in a Straight Fluvial River. 33rd IAHR Congress, Vancouver. 2963-2970.

Tominaga, A. and Matsumoto D. 2006. Diverse riverbed figuration by using skew spur-dike groups, River Flow 2006, 1, Balkema, 683-691.